Digital Image Noise Estimation Using DWT Coefficients

Varad A. Pimpalkhute, Rutvik Page, Ashwin Kothari, *Senior Member, IEEE*, Kishor M. Bhurchandi, *Member, IEEE*, and Vipin Milind Kamble

***Abstract*— Noise type and strength estimation are important in many image processing applications like denoising, compression, video tracking, etc. There are many existing methods for estimation of the type of noise and its strength in digital images. These methods mostly rely on the transform or spatial domain information of images. We propose a hybrid Discrete Wavelet Transform (DWT) and edge information removal based algorithm to estimate the strength of Gaussian noise in digital images. The wavelet coefficients corresponding to spatial domain edges are excluded from noise estimate calculation using a Sobel edge detector. The accuracy of the proposed algorithm is further increased using polynomial regression. Parseval's theorem mathematically validates the proposed algorithm. The performance of the proposed algorithm is evaluated on a standard LIVE image dataset. Benchmarking results show that the proposed algorithm outperforms all other state of the art algorithms by a large margin over a wide range of noise.**

***Index Terms*— Gaussian noise, noise estimation, DWT coefficients, edge detection, polynomial regression.**

I. Introduction

In the modern era of digitization, digital images and documents contribute to a large subset of the generated digital data. The easy availability of cameras, imaging devices, and the ever-decreasing cost of memory has enabled humans to capture images readily. As imaging technology advances, the expectations of the quality of images are also increasing. Although the imaging sensor always tries to capture the fine and exact details in an image, it is inherently accompanied by specific amounts of noise. The strength of this noise is significantly less and frequently not perceivable by the human vision. But in relatively more demanding and convoluted conditions like low ambient light, fast-moving object, etc., the conspicuity of noise increases drastically. There exist many algorithms to drastically remove this noise but they require an accurate estimate of noise present in the image [1] [2] [3] [4]. Thus, the image noise should be estimated accurately in order to obtain noise-free images.

The accurate noise level estimation results in better quality images using denoising algorithms. This is immensely helpful in precision demanding applications like biomedical imaging [5] [6], noise removal in astronomical images [7] and satellite images [8]. A few neural network-based approaches perform the denoising operation without a noise estimate. But the need for noise estimate in these algorithms is compensated by the neural network which requires a lot of training data and the performance is dependent on training efficiency [9].

Noise estimation in digital images has invited a fairly high amount of research attention. It is increasingly finding its applications in different problems and tools of Computer Vision, commercial photography, etc. The estimation of the noise level enables us to find suitable parameters for image denoising and also rating the visual quality of images for commercial applications.

II. Related Work

Noise estimation algorithms can be categorized into spatial domain and transform domain techniques. The spatial domain techniques directly use the pixel values to determine the amount of noise present in an image. These techniques mainly try to exploit the local structural characteristics of image contents. Each pixel is related to at least one of its neighboring pixels in a natural image. The presence of noise disturbs this correlation between adjacent pixels. This deviation is the main indicator of the amount of noise present in an image. On the other hand, transform domain techniques transform the input image into a new domain and the transform coefficients where noise and image characteristics are easily separable are used for noise estimation. This separability of coefficients corresponding to noise and the image content leads to better noise estimation algorithms. But the transform computational overhead increases the computation complexity of these algorithms.

The spatial domain techniques for noise estimation rely totally on the variation of pixel values in the input image. These algorithms either use the complete image information at once or use patch-based statistics to determine the noise estimate. The spatial domain algorithms cannot directly segregate the noise component from the image information accurately. Additionally, the patches with minimum image contents are

Manuscript received February 5, 2020; revised November 5, 2020; accepted December 24, 2020. Date of publication January 13, 2021; date of current version January 20, 2021. The associate editor coordinating the review of this manuscript and approving it for publication was Dr. Pavan Turaga. *(Corresponding author: Varad A. Pimpalkhute.)*

Varad A. Pimpalkhute and Vipin Milind Kamble are with the Department of Electronics and Communication Engineering, Indian Institute of Information Technology, Nagpur (IIITN), Nagpur 440006, India (e-mail: pimpalkhutevarad@gmail.com; vipinkamble97@gmail.com).

Rutvik Page is with the Department of Computer Science and Engineering, Indian Institute of Information Technology, Nagpur (IIITN), Nagpur 440006, India (e-mail: rutvikpage1999@gmail.com).

Ashwin Kothari and Kishor M. Bhurchandi are with the Department of Electronics and Communication Engineering, Visvesvaraya National Institute of Technology, Nagpur (VNIT), Nagpur 440010, India (e-mail: ashwinkothari@ece.vnit.ac.in; bhurchandikm@ece.vnit.ac.in).

Digital Object Identifier 10.1109/TIP.2021.3049961

(a) Lena. (b) Barbara. (c) Cameraman. (d) Peppers.

Fig. 1. Standard images corrupted by noise of standard deviation $\sigma = 20$.

chosen to determine the noise estimate. But this increases the computational cost as the variance of all small image patches need to be calculated to determine the lowest variance patch [10]. This model doesn't give high estimation accuracy for the standard deviation of noise greater than 15. Patch-based algorithms also separate the noise component using techniques like Principal Component Analysis (PCA) [11]. Another technique to estimate noise using patch-based algorithms is to use a threshold to select weak textured patches, i.e. patches with minimum image content. Though this process is computationally strenuous, it results in a better performing algorithm [12]. Another spatial domain approach integrates statistical sampling theory concepts with the Gaussian distribution nature of noise to obtain the noise estimate [13]. This approach uses relatively lesser pixel information as against other algorithms that employ the complete test image for noise estimation.

One of the simplest image noise estimator emerged from the study related to statistics of Gaussian distribution of noise. It was observed that the image noise energy mostly gets confined to high pass wavelet transform coefficients. It was found that even a simple statistical parameter like the median of transform domain coefficients was sufficient to efficiently determine noise present in an image with fair accuracy [14]. Though very simple to use, this method lacked the noise level estimation accuracy for high noise levels ($\sigma > 40$). Researchers tried to improve noise estimation accuracy by slight modifications to the wavelet-based thresholding approach but the improvement in performance was only marginal [15]. Also, it was tested for a limited noise standard deviation range. Along with wavelet transform, Discrete Cosine Transform (DCT) was also used to determine the noise level of an image [16]. In the case of DCT, instead of the commonly used central tendency (median), kurtosis was used as an indicator of the image noise strength. The stability of the performance is unknown as the algorithm was presented for a limited noise range.

The general strategy to save computations is to use small size image patches with minimum variance for noise estimation. It is assumed that these patches have a minimum contribution towards variance due to the image content. A slightly different approach has also been employed where a particle filter is used to find large homogeneous regions in an image [17]. This method lacks the noise level estimation accuracy for high noise levels ($\sigma > 40$). Large heterogeneous image patches can also be used for noise estimation. One such estimator uses Median Absolute Deviation (MAD) of heterogeneous patches to indirectly calculate image noise [18]. Statistical analysis of image patches also revealed that there is a strong correlation between the noise strength and the eigenvalues of the covariance matrix of that patch [19]. On similar lines, image patch eigenvalue distribution of the covariance matrix also provides effective noise estimation [20].

Minimum variance image patches effectively indicate noise as there is a minimum intrusion from image contents. These patches mostly belong to the smooth regions of the image. A signal-dependent noise model was trained from the local mean and variance of these patches to estimate the noise [21]. To further reduce the effect of image contents, boundary blur is used to smooth segmentation edges. Affine reconstruction model is then applied to extract noise strength from the processed patches [22]. The selection of suitable image patches was decided based on the rank of each patch. The low-rank patches along with Principal Component Analysis (PCA) also leads to a fair estimation of noise strength [23].

Other innovative approaches include a finite-difference filter. This method tries to remove the image content which ultimately leaves noise for easier estimation [24]. An interesting observation of Natural Scene Statistics (NSS) is that the variance of normalized DCT coefficients of natural images is scale-invariant. Thus, the presence of noise can be determined by observing the variance of normalized image DCT coefficients [25]. In the case of highly textured images, the lowest energy DCT block of size 8×8 is also used as a measure to determine the noise estimate. This low energy DCT block represents the spatial part of the image where the contribution of texture is minimum [26]. A patch-based DCT approach is suitable to extract the noise component of an image but the performance of such an approach depends on the patch size [27]. DCT also has a property of high kurtosis and scale invariance for natural images. Using this property, the noise component can be calculated using the statistics of DCT coefficients [28]. A training model-based approach using DCT and Wavelet Transform coefficients was also used for noise estimation. In this work, the Generalized Gaussian Distribution is used to fit the transform domain coefficients with respect to the pristine images transform domain coefficients [29].

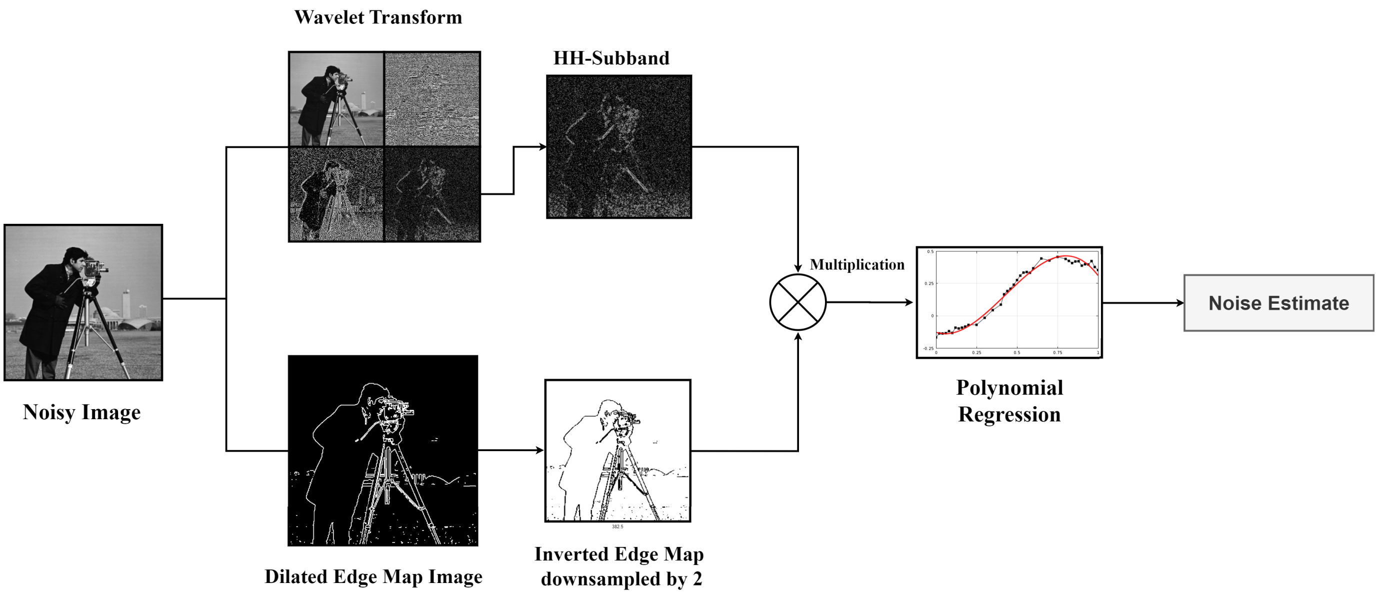

Fig. 2. Proposed method for estimation of noise.

Adaptive estimation of image noise is also possible using Singular Value Decomposition (SVD) tail statistics [30]. This algorithm is specifically designed to achieve higher estimation accuracy at low noise levels ($\sigma \leq 15$) only.

Texture representation tools are also used to select the optimum region of an image for noise estimation. Gabor filter-based techniques use its directional property to represent the color and texture to estimate noise by skipping the invalid pixels [31]. Such approaches try to reduce the computations by filtering out the invalid pixels from noise computation but the pre-processing steps itself add up a significant amount of computational overhead to the algorithm. Scattering transform-based features are also used to extract the texture region from an image. Scattering transform is a translation-invariant descriptor which yields the local texture of an image [32].

The research in the area of noise estimation is limited to the low level of noise and noise estimators for the high magnitude of noise standard deviation ($\sigma > 40$) have not been published widely. The published literature tried to minimize image contents using only minimum variance in the spatial domain and high frequencies in the transform domain. The variations in noise estimates due to image edge magnitudes were overlooked in the published literature. The non-linear relation between noise features and estimates was not considered in the previous work. This resulted in considerably inaccurate noise estimates.

In the recent years, neural network based approaches have emerged to be effective in noise estimation. The neural network based algorithms rely on the extent of training data to obtain an acceptable accuracy. One of the initial attempts of noise estimation used a fuzzy system to process three statistical parameters [33]. It was a basic fuzzy rule based system to optimize the noise estimation problem. Genetic algorithm in combination with Extreme Machine Learning (ELM) is used for estimation of signal dependent noise such as Rice noise [34]. This algorithm shows promising results for accurate noise estimation the accuracy is tested till true noise standard deviation of 30. Another approach assumed that the noise strength affecting each pixel is different and followed a deep convolutional neural network architecture for pixelwise noise estimation [35]. This approach used a stack of customized residual blocks independent of any pooling step. Another recent approach used particle swarm optimization to determine the optimal parameters of Singular Value Decomposition for noise estimation [36].

In this paper, we propose a novel method for the estimation of noise in digital images using edge energy removal from 1^{st} level image DWT coefficients. Our approach utilizes a hybrid of spatial domain edge information suppression and transform domain coefficients' statistics. Polynomial regression is used to compensate for the no-linearity between noise features and noise estimates. Thus the estimation error drastically reduces without the excessive computational overhead and over a wide range of noise standard deviation. A detailed analysis using Parseval's theorem is provided to further strengthen our results.

The paper is organized as follows: Section II gives a brief overview of the past work in this research area. Section III discusses the basics of the wavelet transform, edge detector, and the polynomial regression. Section IV presents the proposed model for the estimation of noise along with the required mathematical analysis. Performance benchmarking is included in Section VI and the paper is concluded in Section VII.

III. Spatial and Transform Domain Operations

The proposed algorithm is a hybrid approach that uses both; spatial as well as transform-domain information. The transform domain information is obtained using the 1^{st} level Discrete Wavelet Transform (DWT) [37]. The spatial characteristics of image are obtained using the Sobel edge detector [38]. The accuracy of the noise estimate is further improved

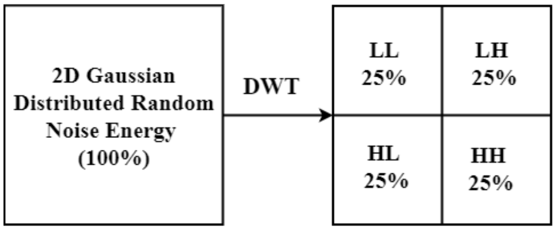

Fig. 3. Energy distribution of Gaussian noise in 2D.

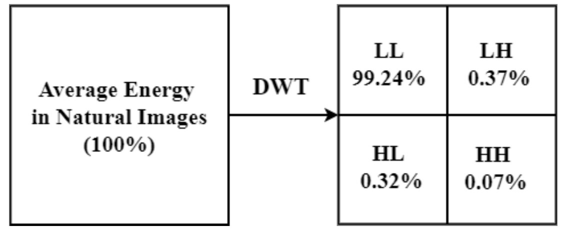

Fig. 4. Average energy distribution of LIVE dataset.

using regression [39]. This section presents a brief introduction to all these topics.

A. Wavelet Transform

Wavelet transform decomposes a signal into its sub-bands using a series of high-pass and low-pass filters. As noise is generally categorized as a high-frequency component, it is easier to separate it from the signal using wavelet transform [37]. The decomposition of frequency content depends on the number of levels of DWT. A signal $x(n)$ can be decomposed into high-pass y_{high} and low-pass y_{low} components using high-pass filter g and low-pass filter h as presented in equation 1.

$$
\begin{aligned}
y_{high}[k] &= \sum_{n} x[n].g[2k-n] \\
y_{low}[k] &= \sum_{n} x[n].h[2k-n]
\end{aligned} \tag{1}
$$

As an image is a two dimensional signal, DWT is applied in parts, i.e., separate filtering operation on rows and columns. As the output of high-pass and low-pass filters contain redundancy and need to have multi-resolution, a down-sampling step is added after filtering. The resulting sub-bands contain horizontal, vertical and diagonal edge information.

The DWT analyzes the signal at different frequency bands with different resolutions by decomposing the signal into coarse approximation and detail information. We use the Haar wavelet as a basis function for decomposing an image into the corresponding sub-bands [40]. Haar wavelet is the simplest wavelet in the wavelet family and can be defined as a step function $\psi(t)$ as,

$$
\psi(t) = \begin{cases} 1 & 0 \leq t < 1/2 \\ -1 & 1/2 \leq t < 1 \\ 0 & otherwise \end{cases} \tag{2}
$$

The reason we are using Haar Wavelet is the use of integral images results in the fast computation of features for any image size. It also provides a simple and efficient approach for analyzing local aspects of a 2D signal.

The sub-band coefficients obtained by decomposing an image using Haar wavelet represent the image content as well as noise. Among the 4 sub-bands, the HH sub-band mainly contains coefficients corresponding to the diagonal edges and noise. Removal of the edge corresponding coefficients from the HH sub-band gives an accurate estimate of noise. Details of the process are presented in Section IV.

B. Edge Detection

Edge Detection is a method of determining boundaries between different objects in an image. It basically operates by detecting discontinuities at the pixel levels in a local neighborhood. Image segmentation and data extraction in image analytical areas like computer vision, image interpretation, etc are achieved using edge detection as a primary tool. The edge detection methods can be roughly categorized into two classes; Gradient and Laplacian.

The difference between these methods branches from the mathematical formulations itself, i.e. the number of derivatives on the image vector. The gradient method works by finding the extremum values of the first derivative of the image. The Laplacian method searches for the zero crossings in the second derivatives of the image to detect edges [41]. Although these essentially represent similar mathematical conditions, different improvements like a change of operators lead to a better quality of edge detection for different applications. Various edge detection operators like Canny, Prewitt, Robert and Sobel have been introduced [42]. Mathematically, for an image function, $f(x, y)$, the gradient magnitude, $g(x, y)$ and the gradient direction, $\Theta(x, y)$ are computed as:

$$
\begin{aligned}
g(x, y) &\cong (\Delta x^2 + \Delta y^2)^{\frac{1}{2}} \\
\Theta(x, y) &\cong atan\left(\frac{\Delta y}{\Delta x}\right)
\end{aligned} \tag{3}
$$

where,

$$\Delta x = f(x+n, y) - f(x-n, y)$$

and,

$$\Delta y = f(x, y+n) - f(x, y-n)$$

In the proposed work, we use the Sobel operator for edge detection. Sobel operator is a more efficient choice for implementability on hardware, as compared to the computationally heavy Laplacian methods. This is backed by the empirical observations obtained using different operators (like Canny, Roberts, Prewitt [42]) during our experiments.

C. Polynomial Regression

Given a set of points, polynomial regression is a process of structuring a graph or a mathematical function, which best accommodates the input points. Again, this structuring might also be subject to certain constraints or parameters, which may or may not affect the basic pattern of the resulting graph or mathematical function. Polynomial regression is one of the

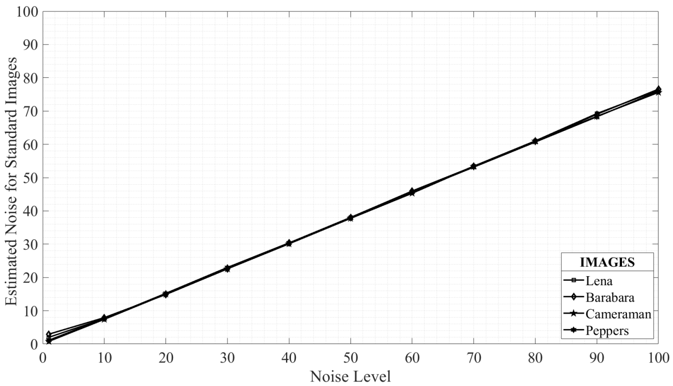

Fig. 5. Estimation before polynomial regression on standard images.

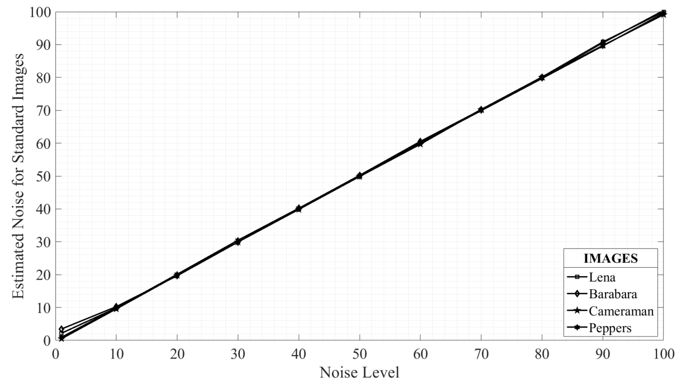

Fig. 6. Estimation after polynomial regression on standard images.

most widely used statistical tools in the research community for handling non-linear system outputs.

Although there are a lot of traditional polynomial regression methods, the one which we use in this paper is the Root Mean Square Error Minimization Method (RMSE). Mathematically let y_i indicate observed value and y_i' indicate the predicted value for the i^{th} observation. With the total number of observations being n, the RMS Error/Deviation [43] is given in,

$$RMSE = \sqrt{\frac{\sum_{i=1}^{n}(y_i' - y_i)^2}{n}} \tag{4}$$

D. Noise Estimation Using DWT

Noise estimation using DWT is a multi-step process. It begins with obtaining an initial estimate using the basic DWT algorithm [14]. This algorithm estimates the Gaussian noise in an image using the median of absolute value of DWT coefficients as in equation 5.

$$\sigma_{DWT} = \frac{median(abs(W))}{0.6745} \tag{5}$$

σ_{DWT} is the image noise estimate obtained from HH sub-bands of 3 level wavelet coefficients represented by W. But the accuracy of this estimate is low due to the presence of coefficients corresponding to diagonal image edges in HH sub-band (W). The accuracy further reduces at higher noise levels.

IV. Proposed Noise Estimation Method

The methodology of the proposed work is based on eliminating the limitations of the basic DWT based algorithm. The maximum energy of diagonal edges and noise present in an image gets concentrated in the HH sub-band of DWT.

Along with noise energy, the HH sub-band also contains coefficients corresponding to the diagonal edges present in the image. This causes an unpredictable noise estimation error as the number of edge pixels varies with each image. We exploit this information by removing the HH sub-band coefficients corresponding to edges. We use the Sobel edge detector [44] to first obtain an edge map of the image. The edge map is down-sampled along rows and columns to match the dimensions of the HH sub-band. A dot product of the HH sub-band and inverted down-sampled edge map gives us the modified HH sub-band that contains coefficients corresponding to only noise. We use the statistics of the modified HH Sub-band coefficients to obtain the initial estimate of noise (σ_{init}). The accuracy of the initial noise estimate is further improved using polynomial regression. The HH sub-band analysis is mathematically backed by Parseval's theorem which equates the energy of a signal in different transform domain representations. We have experimentally validated Parseval's proposition on LIVE dataset images. The energy distribution of natural images is presented in Fig 4. Fig 3 presents the energy distribution of zero-mean Gaussian noise in the four DWT sub-bands. Flowchart of the proposed method is summarized in Fig. 2.

A. Initial Estimate Using DWT

In the proposed algorithm, instead of using median of the DWT HH sub-band coefficients, we use the energy conservation property across different domains to obtain a better noise estimate. An experimental analysis of the same is presented further in this section.

To remove the estimation error caused due to edges, we first obtain the location of edges using a Sobel edge detector in the form of a mask. We then re-size the edge map (EM) to match the size of the HH sub-band (W) obtained using wavelet decomposition. The re-sized edge-map EM_r is achieved by down-sampling the edge-map (EM) by 2 along rows as well as columns. Since a practical edge is rarely single pixel thick, we dilate the edge map so that a better representation of the actual edge width can be obtained. The dilated edge map EM_{rd} is obtained by dilating the edge map (EM) by a constant k as in equation 6.

$$EM_{rd} = EM \oplus k \tag{6}$$

The constant k controls the removal of edge coefficients from the HH sub-band. A lower value of k is unable to remove some of the coefficients corresponding to unsharp edges whereas a higher value of k removes the coefficients corresponding to noise. This leads to an underestimation of noise. The effect of parameter k on the performance of the proposed algorithm is included in Section V.

We obtain an inverted edge-map (EM_{rdi}) from this re-sized dilated edge-map as in equation 7.

$$EM_{rdi} = 1 - EM_{rd} \quad (7)$$

In the re-sized inverted dilated edge-map, spatial domain edge locations are represented by zeros and non-edge locations are represented by ones. This inversion help in directly removing the edge coefficients from the HH sub-band by Hadamard product of HH sub-band coefficients and the inverted re-sized edge-map as presented in equation 8.

$$W_{ne} = W \circ EM_{rdi} \quad (8)$$

W_{ne} represents the HH sub-band coefficients corresponding to non-edge region present in the image.

B. Relation Between DWT Coefficients and Noise Strength

We conducted an experiment to determine the distribution of noise energy in the DWT sub-bands. For this, we generated multiple 2D random variables of size $m \times n$ having Gaussian distributed noise values with standard deviation σ. It was observed that the average noise energy present in the spatial domain gets equally distributed among the four sub-bands in the wavelet domain. Fig 3 represents the average noise energy distribution among the DWT sub-bands. This distribution of energy is in accordance with Parseval's theorem [45] which states that L2 norms of a function in spatial domain and transform domain are equal i.e., the sum of squared values in spatial domain is equal to the sum of squared coefficients in the transform domain. This can be mathematically represented as,

$$\sum_{n=-\infty}^{\infty} |x[n]|^2 = \frac{1}{2}\int_{-\pi}^{\pi} |X(e^{j\omega})|^2 d\omega. \quad (9)$$

Thus extracting noise energy from any one band is sufficient to determine the total noise energy or noise strength.

For an image I corrupted by zero-mean Gaussian noise of standard deviation σ_n, the mean value of the noisy image I_n will not change as the noise is zero mean. In the wavelet domain, the mean value of the image contributes to the LL sub-band. The remaining sub-bands constitute the edge information. As seen in Fig. 3, the noise energy is equally distributed among the sub-bands. Considering only the HH sub-band, the coefficients correspond only to noise and the diagonal edges. As such, extracting noise information from the HH sub-band by simply removing the coefficients corresponding to edges using equation 8 is reliable. In other words, the edge removed HH sub-band (W_{ne}) contains 25% or $1/4^{th}$ of the noise energy as presented in equation 10.

$$\sigma_{n_e}^2 = \frac{4}{N^2} \times \sum_{i,j \in HH} W_{ne}^2(i,j) \quad (10)$$

We observed the energy distribution in the sub-bands in 29 different LIVE dataset images. As seen in Fig. 4, the average energy in the HH sub-band is 0.07% of the total energy of the image. Thus, even on adding this amount of energy to the HH sub-band of noisy matrix in Fig. 3, there will be a negligible change in the overall energy present in the zero mean HH sub-band. Thus, we can validate the correctness of equation 10 for the noise estimate $\sigma_{n_e}^2$.

In terms of standard deviation, equation 10 can be re-written as,

$$\sigma_{n_e} = \frac{2}{N} \times \sqrt{\sum_{i,j \in HH} W_{ne}^2(i,j)} \quad (11)$$

The above equation holds true even though the contents of image are not zero mean. This is because the HH sub-band coefficients correspond only to the edges and noise and are independent of the mean. The basic assumption about noise is it is zero mean and thus it does not add to the mean value of the image.

C. Final Noise Estimation Using Polynomial Regression

The estimated noise obtained using equation 11 yields the initial estimate of noise (σ_{init}). Hence forth, we use σ_{init} as the initial noise estimate.

$$\sigma_{init} = \sigma_{ne} \quad (12)$$

σ_{init} mathematically indicates the total noise that is estimated to be present in the image. In practice, σ_{init} is somewhat different than the actual or true noise. This discrepancy in σ_{init} and the actual or true noise is due to the inaccuracies in edge detection and original image texture that is misinterpreted as noise. The Sobel edge detector does not detect the weak edges present in an image which further contribute to error in noise estimates. Thus, coefficients corresponding to the weak edges remain present in W_{ne} (as in equation 8). It is not possible to have a perfect edge map to solve this problem of detecting all the weak edges. Employing other edge detectors like the Canny edge detector increases the computation cost without any increase in noise estimation accuracy. The presence of texture region information in the HH sub-band coefficients, though very small, causes error in noise estimation, especially at low noise levels. We overcome these limitations using polynomial regression and training procedure explained in Section III.C.

The final noise estimate (σ_{est}) is obtained from the initial noise estimate (σ_{init}) using a simple polynomial equation as in equation 13.

$$\sigma_{est} = p_1\sigma_{init}^4 + p_2\sigma_{init}^3 + p_3\sigma_{init}^2 + p_4\sigma_{init} + p_5 \quad (13)$$

Details of calculating the polynomial coefficients (p_1 to p_5) are illustrated in section V.

Though classical tools like wavelet, Sobel edge detector and regression analysis are used in the proposed algorithm, these tools are very reliable and perform consistently for a diverse range of noise standard deviation. The novelty of the proposed algorithm lies in the combined use of these tools which balance the limitations of each other. The noticeable drop in noise estimation accuracy at low noise level (represented by the DWT coefficients) is compensated by the regression analysis which takes into account the effect of texture region on the noise estimates. The regression analysis also counterbalances for any lack in the performance of the Sobel edge detector as it represents all the possible textures and edges that can

TABLE I
VARIATION IN σ_{est} OVER 100 TRIALS

Variability in Estimation	% error in LIVE dataset images on 100 iterations								Average % error
	Bikes	Caps	House	Lighthouse	Monarch	Ocean	Parrot	Rapids	
Mean Error	0.6918	0.7327	0.7916	0.3931	0.6169	0.8095	0.7656	0.3889	**0.6488**
Standard Deviation Error	0.0554	0.0486	0.0451	0.0383	0.0541	0.0493	0.0544	0.0499	**0.0494**

be present in natural images. Regression also compensates for the saturation in estimate values at higher noise levels. Thus regression addresses the non-linearity at lower as well as higher noise level to yield accurate estimates over a wide range of noise.

D. Contributions of the Paper

The proposed noise estimation algorithm is simple, computationally light and can estimate the noise in real-time. The existing noise estimation algorithms relied solely either on the spatial domain statistics or the transform domain data to estimate the noise. The proposed algorithm makes use of both, spatial as well as transformation domain operations to obtain a reliable estimate of noise. Also, only the level-1 wavelet sub-band coefficients are used thereby reducing the computationally overhead. Another significant contribution of the work is its reliable noise estimation over a wide range of noise standard deviation. The existing algorithms' performance was consistent but only over a limited noise level. The proposed work also experimentally validates that the HH sub-band contains the least amount of signal energy and thus is the most suitable sub-band for noise estimation. The most suitable edge detectors specific for noise estimation are quantitatively determined in the proposed work.

V. EXPERIMENTS, RESULTS AND DISCUSSIONS

The proposed algorithm is validated on standard images from LIVE dataset [46] containing 29 pristine images. The images in LIVE dataset contain a wide variety of objects and structures which are available in day-to-day life. We use the pristine (noise-less) images from the LIVE dataset in our experiment as zero noise images. The proposed noise estimation method is validated on a computer system with the following specifications: Intel(R) Core(TM) i5-7200U processor operating @ 2.50GHz, with 8.00GB RAM on Windows 10 Home operating system using MATLAB.

Before actual validation of the proposed algorithm, the polynomial regression coefficients are obtained using a set of standard images shown in Fig. 1 (lena, barbara, cameraman and peppers) expected to contain a broad variety of real-life textures. Known noise levels (σ_{added}) are added to these images and the initial noise estimates (σ_{init}) are obtained using equation 12. This process is repeated over 100 trials for a wide range of noise levels to obtain a robust σ_{init} vector corresponding to each of the four images. Element wise average of the σ_{init} vectors results in a single vector. This vector along with the added noise level (σ_{added}) vector is used to obtain a mapping function using polynomial regression as discussed in Section III.C. The polynomial coefficients for equation 13 for estimation of Gaussian noise are obtained as shown in equation 14;

TABLE II
EFFECT OF k ON THE ALGORITHM'S PERFORMANCE

k	Average error (%) in noise estimate (σ_{est})			
	Bikes	Caps	Monarch	Rapids
1	1.0579	1.6546	0.8261	0.3944
2	**0.6907**	**0.7739**	**0.6487**	0.3711
3	1.3601	1.2282	0.6642	**0.3510**
4	1.6908	1.0156	1.5882	0.4287
5	1.7541	1.8049	3.0965	0.6768

$$p_1 = -5.089 \times 10^{-08};\ \ p_2 = 1.692 \times 10^{-05};$$
$$p_3 = -0.001871;\ \ p_4 = 1.386;\ \ p_5 = -0.6109; \quad (14)$$

The coefficients obtained using these images ensure maximum robustness and accuracy of the proposed algorithm. The images used to obtain the regression coefficients and the images used for validation are mutually exclusive. The noise estimate before and after the regression are presented in Fig. 5 and Fig. 6 respectively.

The optimum value of edge dilation parameter k is experimentally obtained by varying k and observing the performance of the proposed algorithm on LIVE dataset. The experimental results are presented in Table II. The constant k ensures the optimum removal of coefficients corresponding to edges from HH sub-band. A lower value of k retains some of the coefficients corresponding to edges whereas a higher value of k removes the coefficients corresponding to noise. From Table II, it can be observed that the performance of the proposed algorithm is optimum for $k = 2$ which represents optimum edge energy removal from the HH sub-band.

Any other edge detector can also be used for edge energy removal before noise estimation. A comparative analysis of all the major edge detectors [42] along with Sobel is experimentally carried out and presented in Table IV. The edge detectors yield comparable results. Though the noise estimation error for the Roberts edge detector is minimum, the Sobel edge detector is marginally faster. As the difference in performance

TABLE III
PERFORMANCE OF THE PROPOSED MODEL ON LIVE DATASET FOR GAUSSIAN NOISE ESTIMATION AND % ERROR IN σ_{est}

σ_{added}	Bikes			Caps			House			Lighthouse			Monarch			E_{avg} at σ
	σ_{init}	σ_{est}	E	σ_{init}	σ_{est}	E	σ_{init}	σ_{est}	E	σ_{init}	σ_{est}	E	σ_{init}	σ_{est}	E	
10	8.08	10.47	4.69	7.55	9.75	2.51	7.93	10.27	2.72	7.74	10.02	0.15	7.65	9.89	1.12	2.24
20	14.89	19.66	1.68	15.10	19.94	0.28	15.03	20.22	1.11	14.90	19.68	1.62	15.14	19.99	0.01	0.94
30	22.28	29.52	1.59	22.76	30.15	0.51	22.93	30.37	1.24	22.42	29.70	0.99	22.67	30.03	0.11	0.89
40	29.84	39.49	1.27	30.37	40.18	0.45	30.67	40.59	1.48	30.23	40.01	0.03	30.08	39.80	0.49	0.74
50	37.67	49.75	0.49	38.06	50.25	0.50	38.13	50.35	0.70	37.87	50.01	0.02	37.61	49.67	0.67	0.48
60	45.23	59.60	0.66	45.69	60.21	0.35	45.67	60.18	0.30	45.48	59.92	0.12	45.20	59.57	0.72	0.43
70	53.08	69.81	0.27	53.31	70.11	0.15	53.52	70.38	0.55	53.16	69.92	0.11	52.95	69.64	0.51	0.32
80	60.78	79.82	0.22	61.08	80.21	0.26	61.15	80.30	0.37	60.90	79.97	0.03	60.55	79.52	0.59	0.29
90	68.52	89.89	0.12	68.75	90.19	0.22	68.78	90.24	0.26	68.64	90.04	0.05	68.34	89.66	0.37	0.20
100	75.93	99.55	0.45	75.91	99.52	0.48	76.28	100.02	0.02	76.24	99.96	0.04	76.37	100.13	0.13	0.22
110	83.89	109.56	0.03	83.91	109.88	0.01	83.63	109.62	0.34	84.00	110.11	0.10	83.68	109.69	0.28	0.15
120	91.14	119.47	0.44	91.12	119.44	0.47	91.61	120.09	0.07	91.44	119.86	0.11	91.52	119.96	0.03	0.22
130	99.61	130.59	0.46	99.66	130.67	0.51	98.95	129.72	0.21	98.82	129.56	0.34	99.15	129.99	0.01	0.31
140	106.48	139.65	0.25	106.46	139.62	0.27	107.23	140.63	0.45	107.55	141.05	0.75	106.69	139.93	0.05	0.35
150	114.46	150.15	0.10	114.37	150.04	0.02	113.84	149.34	0.44	114.49	150.20	0.13	114.39	150.07	0.05	0.15
200	152.78	200.08	0.04	152.66	199.34	0.03	152.54	199.78	0.11	159.80	200.10	0.05	153.22	200.65	0.32	0.11
Aver. % Error		0.79			0.44			0.65			0.29			0.34		**0.50**

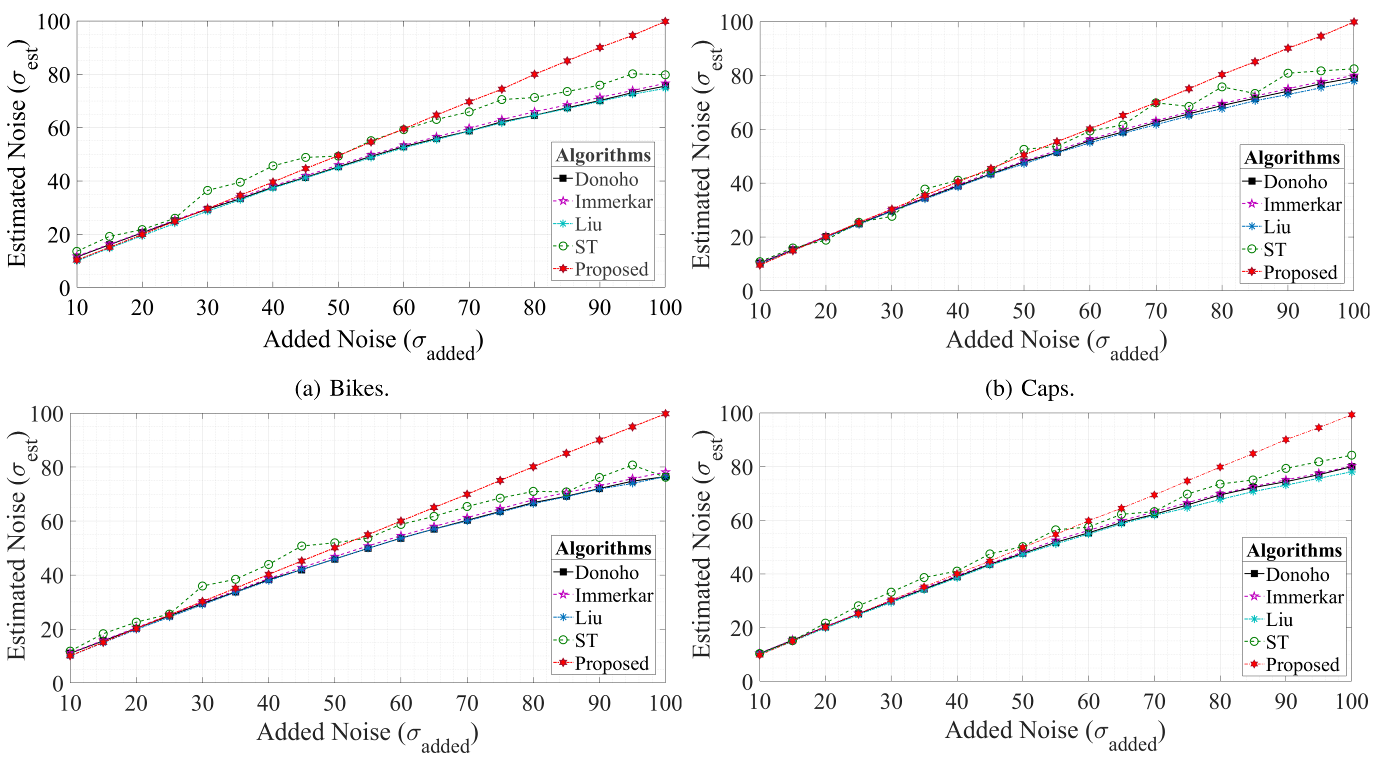

(a) Bikes. (b) Caps. (c) Monarch. (d) Rapids.

Fig. 7. Benchmarking of proposed method on LIVE dataset using average of 100 trials.

is marginal, we chose the Sobel edge detector due to its lower computation time.

For validation of the proposed algorithm, zero-mean Gaussian noise of different standard deviation (σ_{added}) from 10 to 100 are added one by one to the images and the proposed algorithm estimated the noise levels. The accuracy of the proposed algorithm is presented in terms of percent error in noise standard deviation estimation. The quantitative

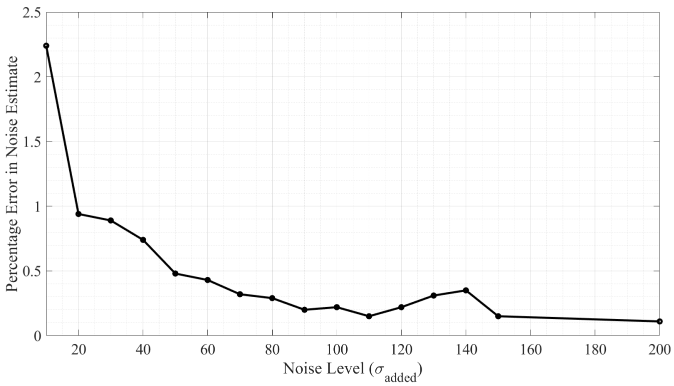

Fig. 8. Average % error in (E_{avg}) in noise estimation vs. σ_{added}.

TABLE IV
PERFORMANCE USING DIFFERENT EDGE DETECTORS

Edge Detector	Average Estimation Error (%)	Average Compute Time (ms)
Sobel	0.50	**55.45**
Canny	1.14	101.22
Roberts	**0.32**	55.63
Prewitt	0.53	61.66

performance of the proposed algorithm is presented in Table III. It can be observed in Table III that there is higher % error at $\sigma_{added} = 10$. This is because natural image textures overlap with noise and also pristine images have inherent noise levels comparable to σ_{added}, thus resulting in high error. The trend in noise estimation error with the increasing noise strength is presented in Fig. 8. It can be observed that the estimation error drastically reduced beyond the noise of standard deviation 20. High noise content destructs image edges and hence there is a slight increase in % error from $\sigma_{added} = 120$ to $\sigma = 140$. After $\sigma_{added} = 140$, the noise content dominates the destroyed edge contents.

The comparative analysis of the proposed algorithm with other state of art algorithms is presented in Table V. For a fair comparison, we use images other than the ones that were used to obtain the polynomial regression coefficients. All the benchmarking algorithms were fed the same noisy images corrupted by noise of the same known standard deviations. The noise strength was gradually increased and the output of all algorithms was noted. We used noise standard deviation (or noise strength) from 10 to 100 in steps of 10. The performance is validated in terms of average % error in noise standard deviation estimation. The % error (E) in noise standard deviation between the added noise level (σ_{added}) and the estimated noise level (σ_{est}) is calculated as in equation 15 and presented in Table V.

$$E = \frac{|\sigma_{added} - \sigma_{est}|}{\sigma_{added}} \times 100 \tag{15}$$

The average error (E_{avg}) in noise standard deviation estimation for all noise levels is indicated in Table V.

TABLE V
BENCHMARKING OF THE PROPOSED METHOD FOR σ_{est}

Algorithm	Avg. Error (%) in σ_{est}			
	Bikes	Caps	Monarch	Rapids
Donoho et al. [14]	5.05	1.27	1.56	3.39
Immerkaer et al. [47]	6.06	1.78	2.45	3.99
Liu et al. [12]	2.79	1.13	0.84	1.32
Kamble et al. (ST) [13]	9.75	7.49	6.28	2.29
Proposed	**2.12**	**0.78**	**0.29**	**0.97**

Part B : E_{avg} for High Noise Levels ($\sigma_{added} > 30$).

Algorithm	Avg. Error (%) in σ_{est}			
	Bikes	Caps	Monarch	Rapids
Donoho et al. [14]	13.93	9.76	9.63	12.58
Immerkaer et al. [47]	12.82	8.82	8.73	11.17
Liu et al. [12]	14.73	10.79	10.62	12.87
Kamble et al. (ST) [13]	5.29	1.69	1.70	1.32
Proposed	**0.83**	**0.37**	**0.34**	**0.24**

TABLE VI
CORRELATION OF PROPOSED METHOD ESTIMATES WITH STANDARD RESULTS ON WHITE NOISE

Algorithm	Correlation
Donoho et al. [14]	0.8959
Immerkaer et al. [47]	0.8971
Liu et al. [12]	0.8878
Kamble et al. (ST) [13]	0.8800
Proposed	**0.9020**

The benchmarking is carried out in two parts: low noise level ($\sigma_{added} \leq 30$) and high noise level ($\sigma_{added} > 30$). At lower levels of noise, performance of the proposed algorithm is comparable to other benchmarking algorithms. But at a higher noise level, the proposed algorithm clearly outperforms all other algorithms.

The variation of E_{avg} against σ_{added} is presented in Fig. 7. It can be observed that the noise estimation of the proposed algorithm is very close to the true value. The consistency of the noise estimation is almost perfect over a wide range of noise.

The proposed algorithm is iterated over 100 times for the complete LIVE dataset of images and the estimated average mean and standard deviation is calculated out to be less than 0.65 and 0.05 respectively as presented in Table I. This highlights the capability of the algorithm to precisely estimate the noise content. Random LIVE dataset images were selected and the average error in estimation for noise from 10 to 100 with a step of 10 was presented in Table V for all algorithms for comparison. It can be seen that the proposed method has much better accuracy than all the other published algorithms.

To prove the consistency of the proposed algorithm, we correlated the algorithm output with known values of noise present in the dataset of images corrupted with white noise provided by the Laboratory of Image and Video Engineering at the University of Texas. We also presented the correlation results of other algorithms on the same dataset in Table VI.

The results in Table VI indicate that the proposed algorithm outperforms the state of art algorithms for all the noisy images present in the LIVE dataset.

VI. Conclusion

We propose a robust and accurate noise estimation method for digital images corrupted by zero-mean Gaussian noise. The proposed method selectively uses the non-edge wavelet transform coefficients to estimate the strength of noise. The edge coefficients are removed using the edge map obtained by Sobel edge detector. The proposed method is mathematically supported by Parseval's theorem of energy conservation. The noise estimate obtained is further improved using polynomial regression. At moderate and high noise levels, the added noise can be precisely estimated. At noise standard deviation of 10, the error in noise estimates is comparatively higher. This is because, at low noise levels, the natural image textures are misinterpreted and considered noise. At the high noise standard deviation of above 100, the image structures like even strong object edges are distorted by noise affecting noise estimation accuracy. The proposed method is computationally light. We benchmarked the proposed method with state of the art algorithms. The proposed method clearly outperforms the existing methods at even less computational cost. The proposed method can be used to bolster the performance of other image processing algorithms like BM3D, object tracking in videos, denoising, etc. by providing an accurate noise estimate. An extension of this work can focus on the estimation of other types of noise using the perceptual quality evaluation.

References

[1] A. Buades, B. Coll, and J.-M. Morel, "A non-local algorithm for image denoising," in *Proc. Comput. Soc. Conf. Comput. Vis. Pattern Recognit. (CVPR)*, vol. 2, 2005, pp. 60–65.

[2] G. R. Easley, D. Labate, and F. Colonna, "Shearlet-based total variation diffusion for denoising," *IEEE Trans. Image Process.*, vol. 18, no. 2, pp. 260–268, Feb. 2009.

[3] L. Sendur and I. W. Selesnick, "Bivariate shrinkage functions for wavelet-based denoising exploiting interscale dependency," *IEEE Trans. Signal Process.*, vol. 50, no. 11, pp. 2744–2756, Nov. 2002.

[4] K. Dabov, A. Foi, V. Katkovnik, and K. Egiazarian, "Image denoising with block-matching and 3D filtering," *Proc. SPIE*, vol. 6064, Oct. 2006, Art. no. 606414.

[5] S. Lahmiri and M. Boukadoum, "Biomedical image denoising using variational mode decomposition," in *Proc. IEEE Biomed. Circuits Syst. Conf. (BioCAS)*, Oct. 2014, pp. 340–343.

[6] S. Aja-Fernández, T. Pieciak, and G. Vegas-Sánchez-Ferrero, "Spatially variant noise estimation in mri: A homomorphic approach," *Med. Image Anal.*, vol. 20, no. 1, pp. 97–184, 2015.

[7] F. Murtagh and J.-L. Starck, "Image processing through multiscale analysis and measurementnoise modeling," *Statist. Comput.*, vol. 10, pp. 95–103, Apr. 2000.

[8] A. K. Bhandari, D. Kumar, A. Kumar, and G. K. Singh, "Optimal sub-band adaptive thresholding based edge preserved satellite image denoising using adaptive differential evolution algorithm," *Neurocomputing*, vol. 174, pp. 698–721, Jan. 2016.

[9] S. Guo, Z. Yan, K. Zhang, W. Zuo, and L. Zhang, "Toward convolutional blind denoising of real photographs," in *Proc. IEEE Conf. Comput. Vis. Pattern Recognit. (CVPR)*, Jun. 2019, pp. 1712–1722.

[10] D.-H. Shin, R.-H. Park, S. Yang, and J.-H. Jung, "Block-based noise estimation using adaptive Gaussian filtering," *IEEE Trans. Consum. Electron.*, vol. 51, no. 1, pp. 218–226, Feb. 2005.

[11] S. Pyatykh, J. Hesser, and L. Zheng, "Image noise level estimation by principal component analysis," *IEEE Trans. Image Process.*, vol. 22, no. 2, pp. 687–699, Feb. 2013.

[12] X. Liu, M. Tanaka, and M. Okutomi, "Estimation of signal dependent noise parameters from a single image," in *Proc. Int. Conf. Image Process.*, Sep. 2013, pp. 79–82.

[13] V. M. Kamble, M. R. Parate, and K. M. Bhurchandi, "No reference noise estimation in digital images using random conditional selection and sampling theory," *Vis. Comput.*, vol. 35, no. 1, pp. 5–21, Jan. 2019.

[14] D. L. Donoho and I. M. Johnstone, "Ideal spatial adaptation by wavelet shrinkage," *Biometrika*, vol. 81, no. 3, pp. 425–455, Sep. 1994.

[15] M. Hashemi and S. Beheshti, "Adaptive noise variance estimation in BayesShrink," *IEEE Signal Process. Lett.*, vol. 17, no. 1, pp. 12–15, Jan. 2010.

[16] D. Zoran and Y. Weiss, "Scale invariance and noise in natural images," in *Proc. 12th Int. Conf. Comput. Vis.*, Sep. 2009, pp. 2209–2216.

[17] M. Ghazal and A. Amer, "Homogeneity localization using particle filters with application to noise estimation," *IEEE Trans. Image Process.*, vol. 20, no. 7, pp. 1788–1796, Jul. 2011.

[18] L. Azzari and A. Foi, "Indirect estimation of signal-dependent noise with nonadaptive heterogeneous samples," *IEEE Trans. Image Process.*, vol. 23, no. 8, pp. 3459–3467, Aug. 2014.

[19] G. Chen, F. Zhu, and P. A. Heng, "An efficient statistical method for image noise level estimation," in *Proc. IEEE Int. Conf. Comput. Vis.*, Dec. 2015, pp. 477–485.

[20] R. Chen and C. Yang, "Noise level estimation for overcomplete dictionary learning based on tight asymptotic bounds," in *Proc. Chin. Conf. Pattern Recognit. Comput. Vis. (PRCV)*. Guangzhou, China: Springer, 2018, pp. 257–267.

[21] X. Liu, M. Tanaka, and M. Okutomi, "Practical signal-dependent noise parameter estimation from a single noisy image," *IEEE Trans. Image Process.*, vol. 23, no. 10, pp. 4361–4371, Oct. 2014.

[22] G. Cui, H. Feng, Z. Xu, Q. Li, and Y. Chen, "No-reference image noise estimation based on noise level accumulation," *Opt. Rev.*, vol. 23, no. 2, pp. 208–219, Apr. 2016.

[23] A. Khmag, A. R. Ramli, S. A. R. Al-haddad, and N. Kamarudin, "Natural image noise level estimation based on local statistics for blind noise reduction," *Vis. Comput.*, vol. 34, no. 4, pp. 575–587, Apr. 2018.

[24] J. P. Kowalski, G. Mikolajczak, and J. Peksinski, "Noise variance estimation in digital images using finite differences filter," in *Proc. 41st Int. Conf. Telecommun. Signal Process. (TSP)*, Jul. 2018, pp. 1–4.

[25] P. Gupta, C. Bampis, Y. Jin, and A. Bovik, "Natural scene statistics for noise estimation," in *Proc. IEEE Southwest Symp. Image Anal. Interpretation (SSIAI)*, Apr. 2018, pp. 85–88.

[26] M. Ponomarenko, N. Gapon, V. Voronin, and K. Egiazarian, "Blind estimation of white Gaussian noise variance in highly textured images," *Electron. Imag.*, vol. 2018, no. 13, pp. 1–382, 2018.

[27] S. B. Mohan, T. A. Raghavendiran, and R. Rajavel, "Patch based fast noise level estimation using DCT and standard deviation," *Cluster Comput.*, vol. 22, no. S6, pp. 14495–14504, Nov. 2019.

[28] G. Zhai and X. Wu, "Noise estimation using statistics of natural images," in *Proc. 18th IEEE Int. Conf. Image Process.*, Sep. 2011, pp. 1857–1860.

[29] M. M. Ghazi and H. Erdogan, "Image noise level estimation based on higher-order statistics," *Multimedia Tools Appl.*, vol. 76, no. 2, pp. 2379–2397, Jan. 2017.

[30] E. Turajlic, "Adaptive SVD domain-based white Gaussian noise level estimation in images," *IEEE Access*, vol. 6, pp. 72735–72747, 2018.

[31] S. Jeschke, D. Cline, and P. Wonka, "Estimating color and texture parameters for vector graphics," *Comput. Graph. Forum*, vol. 30, no. 2, pp. 523–532, Apr. 2011.

[32] S. Minaee, A. Abdolrashidi, and Y. Wang, "Iris recognition using scattering transform and textural features," in *Proc. IEEE Signal Process. Signal Process. Edu. Workshop (SP/SPE)*, Aug. 2015, pp. 37–42.

[33] M. Salmeri, A. Mencattini, E. Ricci, and A. Salsano, "Noise estimation in digital images using fuzzy processing," in *Proc. Int. Conf. Image Process.*, vol. 1, 2001, pp. 517–520.

[34] X. Yang, K. Xu, S. Xu, and P. X. Liu, "Image noise level estimation for rice noise based on extended ELM neural network training algorithm," *IEEE Access*, vol. 7, pp. 1943–1951, 2019.

[35] H. Tan, H. Xiao, S. Lai, Y. Liu, and M. Zhang, "Pixelwise estimation of signal-dependent image noise using deep residual learning," *Comput. Intell. Neurosci.*, vol. 2019, pp. 1–12, Sep. 2019.

[36] H. Prasetyo and U. Salamah, "Swarm intelligence for additive white Gaussian noise level estimation," *Int. J. FUZZY Log. Intell. Syst.*, vol. 20, no. 3, pp. 169–180, Sep. 2020.

[37] I. Daubechies, "The wavelet transform, time-frequency localization and signal analysis," *IEEE Trans. Inf. Theory*, vol. 36, no. 5, pp. 961–1005, Sep. 1990.

[38] I. Sobel, "An isotropic 3×3 image gradient operator," Stanford A.I., New Brunswick, NJ, USA, Tech. Rep. 1, Feb. 2014.

[39] P. Lancaster and K. Salkauskas, "Curve fitting with polynomials," in *Curve and Surface Fitting: An Introduction*. New York, NY, USA: Academic, 1995, pp. 29–62.

[40] R. S. Stanković and B. J. Falkowski, "The Haar wavelet transform: Its status and achievements," *Comput. Electr. Eng.*, vol. 29, no. 1, pp. 25–44, Jan. 2003.

[41] D. Ziou and S. Tabbone, "Edge detection techniques—An overview," *Pattern Recognit. Image Anal. C/C Raspoznavaniye Obrazov I Analiz Izobrazhenii*, vol. 8, no. 4, pp. 537–559, 1998.

[42] G. Shrivakshan and C. Chandrasekar, "A comparison of various edge detection techniques used in image processing," *Int. J. Comput. Sci. Issues (IJCSI)*, vol. 9, no. 5, p. 269, 2012.

[43] *Stanford CSE Courses by Dr. Susan*. Accessed: May 25, 2019. [Online]. Available: http://statweb.stanford.edu/~susan/courses/s60/split/node60.html

[44] O. R. Vincent and O. Folorunso, "A descriptive algorithm for Sobel image edge detection," in *Proc. Informing Sci. IT Edu. Conf. (InSITE)*, vol. 40, 2009, pp. 97–107.

[45] D. P. Percival, "On estimation of the wavelet variance," *Biometrika*, vol. 82, no. 3, pp. 619–631, 1995.

[46] H. Sheikh, Z. Wang, L. Cormack, and A. Bovik, "Live image quality assessment database release 2," Lab. Image Video Eng., Univ. Texas Austin, Austin, TX, USA, Tech. Rep. 1, 2005.

[47] J. Immerkær, "Fast noise variance estimation," *Comput. Vis. Image Understand.*, vol. 64, no. 2, pp. 300–302, Sep. 1996.

Varad A. Pimpalkhute is currently pursuing the bachelor's degree with the Department of Electronics and Communication Engineering, Indian Institute of Information Technology, Nagpur (IIITN). His research interests include image processing, meta-learning, and performance optimization.

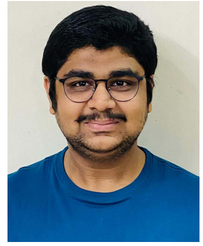

Rutvik Page is currently pursuing the B.E. degree with the Department of Computer Science and Engineering, Indian Institute of Information Technology, Nagpur, India (IIITN). He is currently serving as a Ginsberg Ingermann Research Assistant with the Computational Social Choice and Multi-Agent Systems Laboratory, Ben Gurion University of the Negev, Israel. His research interests include image processing, multi-agent systems, and algorithmic game theory.

Ashwin Kothari (Senior Member, IEEE) received the B.E. and M.Tech. degrees in electronics engineering in 1994 and 2005, respectively, and the Ph.D. degree from the Visvesvaraya National Institute of Technology, Nagpur, India, in 2010. He is currently working as an Associate Professor with the Visvesvaraya National Institute of Technology. He is one of the Coordinators for the Center of Excellence on Commbedded Systems: Hybridization of Communications and Embedded Systems under World Bank assisted project of TEQIP. He has several publications and has contributed book chapters for reputed publications to his credit. He has 26 years of experience in teaching. His research interests include image processing, antennas and wave propagation, electromagnetic, communication, and rough sets.

Kishor M. Bhurchandi (Member, IEEE) received the B.Eng. and M.Eng. degrees in electronics engineering in 1990 and 1992, respectively, and the Ph.D. degree from the Visvesvaraya Regional College of Engineering, Nagpur University, Nagpur, India, in 2002. He is currently working as a Professor with Nagpur University. He is the coauthor of a popular book titled *Advanced Microprocessors and Peripherals* published by McGraw Hill, India. His research interests include color image processing, computer vision, and digital signal processing.

Vipin Milind Kamble received the B.Tech. and Ph.D. degrees in electronics and communication engineering from the Visvesvaraya National Institute of Technology (VNIT), Nagpur, India, in 2011, and the M.Tech. degree in electrical engineering from the National Institute of Technology, Rourkela, India, in 2013. He is currently working as an Assistant Professor with the Department of Electronics and Communication Engineering, Indian Institute of Information Technology, Nagpur. His research interests include noise estimation, image denoising, and image quality assessment.